THE JOURNAL OF BIOLOGICAL CHEMISTRY
Vol. 277, No. 48, Issue of November 29, pp. 46669–46675, 2002
Printed in U.S.A.
© 2002 by The American Society for Biochemistry and Molecular Biology, Inc.

Insight into the Catalytic Mechanism of *Pseudomonas aeruginosa* Exotoxin A

STUDIES OF TOXIN INTERACTION WITH EUKARYOTIC ELONGATION FACTOR-2*

Received for publication, July 10, 2002, and in revised form, August 19, 2002
Published, JBC Papers in Press, September 20, 2002, DOI 10.1074/jbc.M206916200

Souzan Armstrong‡, Susan P. Yates§, and A. Rod Merrill¶

From the Guelph-Waterloo Centre for Graduate Work in Chemistry and Biochemistry, Department of Chemistry and Biochemistry, University of Guelph, Ontario N1G 2W1, Canada

The molecular nature of the protein-protein interactions between the catalytic domain from *Pseudomonas aeruginosa* exotoxin A (PE24H) and its protein substrate, eukaryotic elongation factor-2 (eEF-2) were probed using a fluorescence resonance energy transfer method. Single cysteine mutant proteins of PE24H were prepared and site-specifically labeled with the donor fluorophore IAEDANS (5-(2-iodoacetylaminoethylamino)-1-napthalenesulfonic acid), whereas eEF-2 was labeled with the acceptor fluorophore fluorescein. The association was found to be independent of ionic strength and of the co-substrate, NAD^+ but dependent upon pH. The lack of requirement for NAD^+ to produce the toxin-eEF-2 complex demonstrates that the catalytic process is a random order mechanism, thereby disputing the current model. The previously observed pH dependence for catalytic function can be assigned to the toxin-eEF-2 binding event, as the pH dependence of binding observed in this study showed a strong correlation with enzymatic activity. The ability of the toxin to bind eEF-2 with bound GTP/GDP was assessed using nonhydrolyzable analogues. The results from the substrate binding and catalytic activity experiments indicate that PE24H is able to interact and bind with eEF-2 in all of its guanyl nucleotide-induced conformational states. Thus, the toxin ribosylates eEF-2 regardless of the nucleotide-charged state of eEF-2. These results represent the first detailed characterization of the molecular details and physiological conditions governing this protein-protein interaction.

Pseudomonas aeruginosa is a Gram-negative, rod-shaped aerobic bacterium that is found ubiquitously in the environment (1) and is an opportunistic human pathogen that secretes a number of potent virulence factors, including exotoxin A (ETA).[1] The production of ETA by this bacterium, along with many other virulence factors, allows it to adapt to quite diverse environments including soil, water, sewage, and hospitals. Patients at a high risk for bacterial colonization and subsequent infection include those who are jeopardized by extreme youth or age, severe trauma, AIDS, burns, cystic fibrosis, and cancer (2).

ETA belongs to the family of enzymes termed mono(ADP-ribosyl)transferases and is more specifically a NAD^+-diphthamide ADP-ribosyltransferase (EC 2.4.2.36) (3, 4). ETA, a 66-kDa extracellular protein (5), enters eukaryotic cells by receptor-mediated endocytosis (6) and once it has reached the cytoplasm catalyzes the ADP-ribosylation of its target protein, eukaryotic elongation factor-2 (eEF-2) (7). This ADP-ribosylation reaction inactivates eEF-2 resulting in the inhibition of protein synthesis and ultimately leading to cellular death (5, 8).

The three-dimensional structure of ETA shows that it consists of three distinct functional domains: receptor-binding (domain I), translocation (domain II), and catalysis (domain III) (9, 10). The catalytic domain (residues 400–613) is responsible for the inactivation of eEF-2 by catalyzing the transfer of the ADP-ribosyl moiety from NAD^+ to eEF-2. It is proposed that initially a binary complex forms between NAD^+ and the catalytic domain followed by the subsequent binding of eEF-2, representative of an ordered sequential reaction (11, 12). In addition, stereochemical and kinetic data suggest that the reaction mechanism is likely an S_N1 nucleophilic substitution involving an oxocarbonium cation, despite the observed inversion of configuration for the glycosidic bond formed between the ribose and diphthamide (5, 11, 13, 14). This inversion most likely results because the anomeric carbon of the nicotinamide ribose is susceptible to a backside nucleophilic attack from the N-1 of the imidazole portion of diphthamide (5).

The important catalytic residues for ETA are Glu-553, His-440, Tyr-481, and Tyr-470, which were identified by structural and mutagenesis studies (9, 13, 34, 35). The structure of the catalytic domain shows that the imidazole side chain of His-440, located at the base of the active site cleft, hydrogen bonds with the AMP ribose moiety of NAD^+ and with the main chain carbonyl of Tyr-470 (13). The nicotinamide ring stacks with Tyr-481 and Tyr-470 and is located near the nicotinamide where it is involved in Van der Waals interactions with the thiazole-ribose moiety of the nonhydrolyzable NAD^+ analogue, β-TAD. Glu-553 forms a hydrogen bond with the oxygen of the

* This work was supported by a grant from the Canadian Institutes of Health Research (A. R. M.). The costs of publication of this article were defrayed in part by the payment of page charges. This article must therefore be hereby marked "*advertisement*" in accordance with 18 U.S.C. Section 1734 solely to indicate this fact.

‡ Present address: Photon Technology International, 347 Consortium Court, London, Ontario N6E 2S8, Canada.

§ Recipient of a predoctoral scholarship from the Canadian Cystic Fibrosis Foundation.

¶ To whom correspondence should be addressed. Tel.: 519-824-4120 (ext. 3806); Fax: 519-766-1499; E-mail: merrill@chembio.uoguelph.ca.

[1] The abbreviations used are: ETA, exotoxin A; β-TAD, β-methylenethiazole-4-carboxamide adenine dinucleotide; 5-AF, 5-acetamide fluorescein; ADPRT, ADP-ribosyltransferase; AEDANS, 5-(2-aminoethylamino)-1-naphthalenesulfonic acid; bis-Tris, bis(2-hydroxyethyl)iminotris(hydroxymethyl)methane; CAPS, 3-(cyclohexylamino)-1-propanesulfonic acid; IAEDANS, 5-(2-iodoacetylaminoethylamino)-1-napthalenesulfonic acid; eEF-2, eukaryotic elongation factor-2; eEF-2-AF, 5-AF labeled eEF-2; FRET, fluorescence resonance energy transfer; GDP-β-S, guanosine 5′-*O*-(2-thiodiphosphate); GTP-γ-S, guanosine 5′-*O*-(3-thiotriphosphate); K_A, substrate binding (association) constant; K_D, substrate binding (dissociation) constant; *o*-GTP, oxidized GTP; PE24H, *Pseudomonas aeruginosa* exotoxin A, 24-kDa C-terminal fragment containing a hexa-His tag.

This is an Open Access article under the CC BY license.

thiazole-ribose of β-TAD (11, 13) and may serve to cradle NAD^+ in a reactive conformation, exposing the anomeric carbon for attack by the diphthamide of eEF-2 while still allowing the inversion of configuration at this carbon. Additionally, the negatively charged carboxylate of Glu-553 may stabilize a positively charged reaction intermediate (13).

eEF-2 is a single polypeptide chain with a molecular mass ranging from 90 to 110 kDa depending on the source of its isolation (15). eEF-2 is a factor involved in the elongation phase of protein synthesis and is a member of the GTPase superfamily. Specifically, eEF-2 is responsible for catalyzing the translocation of the peptidyl-tRNA from the A-site to the P-site within the ribosome, movement of the deacylated tRNA from the P-site to the E-site, and finally movement of the mRNA to allow the next codon to be placed in the A-site (16). eEF-2 contains a post-translationally modified histidine residue, 2-[3-carboxyamido-3-(trimethylammonio)propyl]histidine, referred to as diphthamide (17, 18). This residue is located at position 715 in the rat liver eEF-2 sequence near the C terminus of the protein (19). Diphthamide has only been found in eEF-2 and is completely conserved throughout all eukaryotic and archaebacterial evolution (18, 20). Although the diphthamide is the site of toxin attack, it does not appear to be necessary for normal eEF-2 function.

Currently, no three-dimensional structure has been reported for eEF-2, which may help to explain the lack of understanding regarding the toxin-eEF-2 interaction. The aim of the present study was to investigate the physiological conditions requisite for the interaction between eEF-2 and the catalytic domain of ETA using a fluorescence resonance energy transfer (FRET) approach. We introduced single cysteine residues into the catalytic domain of ETA and labeled the domain with a donor fluorophore, whereas the protein substrate, eEF-2 was labeled with the acceptor fluorophore. The integrity of the labeled toxins was assessed through enzyme activity and substrate binding measurements. Furthermore, the dissociation constant for eEF-2 binding to the toxin was also determined. This binding event was shown to be pH-dependent but insensitive to the ionic strength of the aqueous environment and to the presence of the substrate, NAD^+. Finally, the importance of the conformation of eEF-2 on toxin ADP-ribosylation activity was evaluated using GTP and GDP nonhydrolyzable analogues.

EXPERIMENTAL PROCEDURES

Overexpression and Purification of PE24H—The catalytic fragment of ETA with a C-terminal 6-His tag (PE24H) was overexpressed and purified as described (21) except that all cysteine-containing mutant proteins required the chelate-agarose affinity column to be charged with 100 mM $ZnSO_4$.

Purification of eEF-2—eEF-2 was purified from wheat germ as previously described (21) with some modifications.

Site-directed Mutagenesis—Single cysteine mutant proteins were created using either Kunkel mutagenesis (22) or by standard QuikChange™ mutagenesis (Stratagene, La Jolla, CA). The DNA template was the plasmid pPH1 containing the gene for wild-type PE24H. The desired mutation, determined by dideoxy sequencing with an ABI Prism Model 377 DNA sequencer using dye termination and cycle sequencing, was analyzed on a 4.5% acrylamide gel.

Fluorescence Labeling of PE24H—The PE24H protein was labeled with the fluorophore IAEDANS as detailed earlier (8) with some modifications. The labeling efficiency, based on the appropriate absorbance and molar extinction coefficients of the bound fluorophore and the measured protein, ranged between 80 and 100%, with the exception of S408C, which was only 60%.

Fluorescence Labeling of eEF-2—Purified wheat germ eEF-2 protein was labeled with 5-iodoacetamide fluorescein as described previously (8) with some modifications.

Fluorescence and Spectroscopic Measurements—All steady-state fluorescence measurements were obtained using a PTI Alphascan spectrophotometer interfaced with a computer using Felix™ Version 1.21 software (Photon Technology International, South Brunswick, NJ) and equipped with a water-jacketed sample chamber set to 25 °C. The exceptions were the determination of the pH profile for eEF-2 binding and the effects of guanyl nucleotides on binding, for which we used a Cary Eclipse fluorometer (Varian, Mississauga, Ontario, Canada) equipped with a Peltier thermostatted multicell holder at 25 °C. The PE24H-AEDANS excitation (λ_{em} = 480 nm) and emission spectra (λ_{ex} = 337 nm) were recorded for proteins in 50 mM NaCl, 20 mM Tris-HCl (pH 7.9) solution. The eEF-2-AF excitation (λ_{em} = 515 nm) and emission spectra (λ_{ex} = 492 nm) were obtained for proteins in 100 mM KCl, 20 mM Tris-HCl (pH 7.9) buffer.

Absorbance spectra were obtained at room temperature with a PerkinElmer λ-6 double beam, scanning absorption spectrometer (PerkinElmer Life Sciences) interfaced to a personal computer. PE24H-AEDANS absorbance spectra were scanned from 260 to 400 nm in 50 mM NaCl, 20 mM Tris-HCl (pH 7.9) solution. eEF-2-AF absorbance spectra were recorded from 250 to 600 nm in 300 mM KCl, 20 mM Tris-HCl (pH 7.9) buffer.

Fluorescence-based ADPRT Assay—The NAD^+-dependent ADPRT activity for the various cysteine PE24H proteins and their corresponding protein adducts was determined as described by Armstrong and Merrill (21).

The effect of GTP- and GDP-bound eEF-2 was assessed with the substrates ε-NAD^+ (500 μM) GTP-γ-S, and eEF-2 (14 μM; with or without bound guanyl nucleotides) held at saturating levels. The assay was as described above except that the nucleotides (GDP-β-S at 50 μM, Sigma) were initially allowed to bind to eEF-2 for 10 min at 25 °C and the reaction buffer was supplemented with 8 mM $MgCl_2$.

Quenching of Intrinsic Protein Fluorescence—The NAD^+-dependent quenching of the intrinsic tryptophan fluorescence in PE24H was used to determine the binding constant (K_D) for NAD^+ as described elsewhere (5).

Fluorescence-based eEF-2 Binding Assay—The FRET-based assay was conducted as described previously (8). The dissociation constant for eEF-2 binding with PE24H was determined using the following equation as part of the nonlinear fitting function of Origin 6.1 (OriginLab, Northampton, MA): $\Delta F_i/\Delta F_{max} = ([\text{eEF-2}] \times B_{max})/(K_D + [\text{eEF-2}])$, where ΔF_i is the change in fluorescence intensity for each ligand (eEF-2) concentration upon macromolecular association, ΔF_{max} is the maximum change in fluorescence intensity at saturation of the ligand-binding site within PE24H, K_D is the dissociation constant for the binding of eEF-2 with PE24H, and B_{max} is the total PE24H concentration (number of binding sites, as there is 1 site/protein).

S585C-AEDANS was chosen as the control protein to evaluate the effects of NAD^+, urea, salt, pH, and guanyl nucleotides on toxin-eEF-2 binding. S585C and its adduct behave similarly to the wild-type enzyme in terms of its catalytic activity and NAD^+ binding; also this protein labeled with IAEDANS at a high efficiency.

The requirement of NAD^+ for protein complexation was evaluated using the nonhydrolyzable analogue, β-TAD, at a concentration of 200 μM. The ability of denatured PE24H-AEDANS to bind eEF-2-AF was evaluated in buffer containing 4 M urea (Pierce), which denatures the PE24H protein but does not unfold the eEF-2 protein.

The effect of various anions on eEF-2 binding to PE24H was measured by varying the salt concentration from 0 to 800 mM in the binding buffer. The Tris-HCl buffer (20 mM, pH 7.9) was supplemented with KCl, Na_2SO_4, or NaF.

The effect of pH on the binding was obtained by varying the pH between 4 and 12. The buffer contained 50 mM NaCl, and the buffering components (pH range shown in parentheses) were sodium acetate (30 mM, pH 4), bis-Tris (30 mM, pH 6.5–6.8), Tris-HCl (30 mM, pH 7–8.8), and CAPS (30 mM, pH 9–12). The K_D values were converted to K_A values for plotting purposes using the expression, $K_A = 1/K_D$.

The effects of guanyl nucleotides bound to eEF-2-AF was assessed in 50 mM NaCl, 20 mM Tris-HCl (pH 7.9) supplemented with 8 mM $MgCl_2$ with either 50 μM GTP-γ-S or GDP-β-S (Sigma). eEF-2-AF was preincubated with the nonhydrolyzable guanyl nucleotides (at 50 μM) for 10 min before titration with the toxin. The saturating concentration of these nucleotides is near 50 μM (23).

RESULTS

Characterization of the Single Cysteine Mutant Proteins and Their Derivatives—Intrinsic fluorescence-based techniques for studying the interactions between PE24H and eEF-2 have proved difficult because both proteins possess tryptophan fluorescence. The catalytic domain of ETA, PE24H, does not contain any native cysteine residues. Therefore, single cysteine residues were introduced into the protein at defined sites

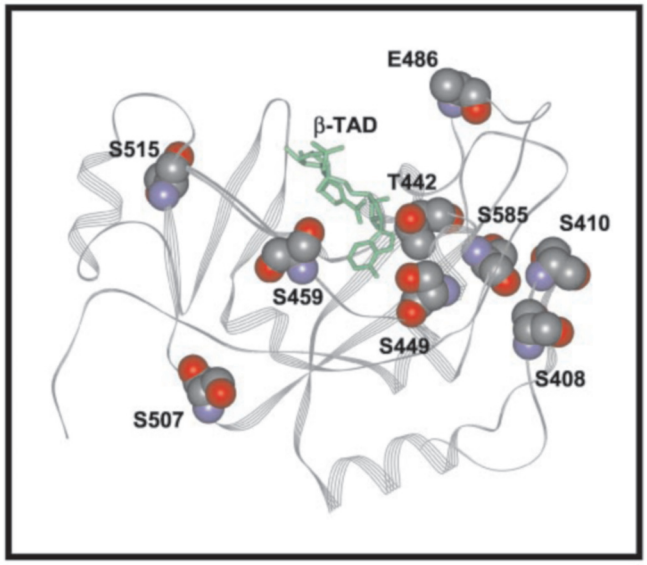

FIG. 1. **Structure of the catalytic domain of ETA complexed with β-TAD.** The protein backbone is shown in *ribbon* format, and the β-TAD substrate is drawn in *stick* form. The sites that were substituted with cysteine residues by site-directed mutagenesis are shown as *space-filled structures*. The model was prepared with the desktop PC modeling package, WebLab Viewer Pro, Version 4.0 (Accelrys, Inc., San Diego, CA). The full coordinates of the catalytic domain of PE24/β-TAD complex (13) (PDB entry, 1AER) were obtained from the *Protein Data Bank, Research Collaboratory for Structural Bioinformatics, Rutgers University* (http://www.rcsb.org/pdb/).

within the toxin. The sites chosen for mutagenesis included those that surround the NAD^+-binding site as well as surface-exposed sites distant from the active site (Fig. 1). All mutant proteins were used to assess the interactions between the toxin and eEF-2. The thiol-specific reaction between the cysteine residues within PE24H and the fluorophore, IAEDANS, created proteins that contained a single, covalently linked reporter fluorophore. AEDANS was chosen as the fluorophore because of its large Stokes shift and because it has an emission spectrum that overlaps well with the absorbance of other fluorescent dyes such as fluorescein. AEDANS is ideal for FRET experiments of up to ~60 Å (24).

The structural integrity of the mutant PE24H proteins with and without the attached fluorophore was assessed by both NAD^+ substrate binding and ADPRT enzymatic activity. None of the single cysteine replacements in PE24H led to significant changes in either the affinity for the NAD^+ substrate or in ADPRT activity (Table I). Generally, introduction of the fluorophore also did not cause major perturbations of the proteins as reflected by measurements of the transferase and binding activities of the mutant adduct proteins (Table II). However, T442C-, S449C-, and E486C-AEDANS showed reduced ADPRT activity upon alkylation (84-, 16-, and 12-fold decrease, respectively) (Table II). Thr-442, situated on the same β-strand as His-440, and Ser-449, located in an α-helix near the opening of the active site cleft, both hydrogen bond with NAD^+ (11, 13) (Fig. 1) and furthermore, Glu-486 is present in the loop region, which was previously identified as modulating the transferase activity of the toxin (8) (Fig. 1). Therefore, the decreased activity of these three mutant proteins is likely a reflection of the spatial importance of these residues for catalytic function; when the AEDANS fluorophore is present at these sites within the corresponding protein adducts, it may sterically interfere with normal enzyme function.

A typical UV-visible absorption spectrum for PE24H-AEDANS is shown in Fig. 2*A*. It is characterized by maxima at 260, 285, and 337 nm; the latter peak was used to determine

TABLE I

Comparison of the ADPRT activity and NAD^+-binding affinity for the cysteine replacement mutants

The kinetics and binding data were determined as described under "Experimental Procedures" and represent the mean ± S.D. of three independent experiments.

Protein	k_{cat}	$K_{D(NAD+)}$
	min^{-1}	μM
Wild type	675 ± 85	55 ± 6
S408C	630 ± 108	59 ± 3
S410C	184 ± 31	50 ± 6
T442C	132 ± 33	35 ± 3
S449C	234 ± 42	129 ± 7
S459C	310 ± 113	55 ± 10
E486C	930 ± 127	57 ± 8
S507C	1256 ± 61	63 ± 2
S515C	307 ± 78	48 ± 5
S585C	731 ± 145	61 ± 4

TABLE II

Comparison of the ADPRT activity, NAD^+, and eEF-2 binding for the cysteine replacement mutants labeled with the fluorophore IAEDANS

The kinetics and binding data were determined as described under "Experimental Procedures" and represent the mean ± S.D. of three independent experiments.

Protein	k_{cat}	$K_{D(NAD+)}$	$K_{D(eEF-2)}$
	min^{-1}	μM	μM
Wild type	675 ± 85	55 ± 6	NA[a]
S408C-AEDANS	435 ± 43	44 ± 10	1.2 ± 0.3
S410C-AEDANS	367 ± 65	51 ± 11	0.9 ± 0.1
T442C-AEDANS	8 ± 1	5300 ± 300	1.2 ± 0.1
S449C-AEDANS	43 ± 7	546 ± 14	0.9 ± 0.1
S459C-AEDANS	542 ± 66	36 ± 4	0.9 ± 0.1
E486C-AEDANS	56 ± 5	115 ± 4	0.8 ± 0.2
S507C-AEDANS	268 ± 30	30 ± 4	1.1 ± 0.2
S515C-AEDANS	396 ± 73	87 ± 15	1.0 ± 0.1
S585C-AEDANS	192 ± 61	30 ± 3	1.9 ± 0.2

[a] Not applicable, as wild-type PE24H contains no endogenous cysteine and therefore cannot be labeled and studied in the FRET-based eEF-2 binding assay. However, an independent eEF-2 binding assay involving the incorporation of 5-hydroxytryptophan into the wild-type PE24H protein gave a K_D for eEF-2 of 0.98 ± 0.06 μM (27).

the labeling stoichiometry of the various PE24H-AEDANS adducts. Also, the fluorescence spectra for PE24H-AEDANS (Fig. 2*C*) show excitation and emission maxima for PE24H-AEDANS at 337 and 480 nm, respectively.

Characterization of eEF-2-AF—Alkylation of eEF-2 using 5-iodoacetamide fluorescein was stringently controlled to ensure that only one label was present per protein molecule. The UV-visible absorption spectrum of eEF-2-AF is characterized by two absorption maxima at 280 and 490 nm (Fig. 2*B*). The fluorescence spectra (Fig. 2*D*) show excitation and emission maxima at 492 and 515 nm, respectively. Introducing a fluorescence moiety into eEF-2 leads to a 4-fold loss in its ability to act as a substrate in the ADPRT assay with wild-type PE24H as the enzyme (data not shown).

FRET-based Binding Assay—The fluorescence emission spectrum of the PE24H-AEDANS fluorophore significantly overlaps with the absorption spectrum of eEF-2-AF; therefore, these fluorophores are a good donor-acceptor pair for FRET studies involving PE24H and eEF-2 (Fig. 2, *B* and *C*).

The protein-protein interactions of these two proteins were measured by FRET between the AEDANS moiety in PE24H (donor) and the fluorescein fluorophore associated with eEF-2 (acceptor). The energy transfer is evident in Fig. 3*A*, as the emission for PE24H-AEDANS was monitored as a function of labeled eEF-2 concentration. A plot showing the binding isotherm for PE24H-AEDANS with eEF-2-AF is shown in Fig. 3*B*, which is indicative of specific, saturable binding between these two proteins. In addition, the binding was

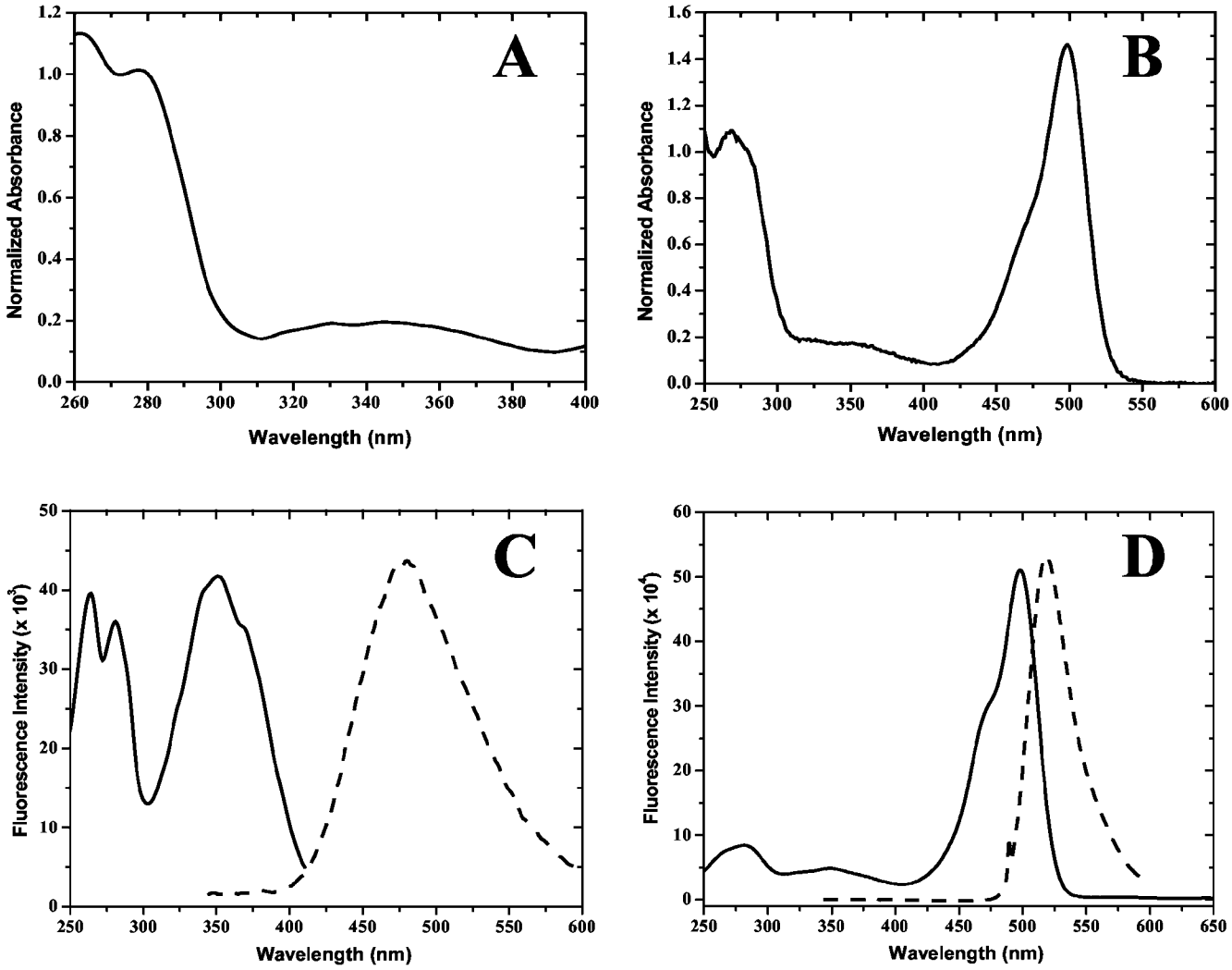

FIG. 2. **Absorbance and fluorescence spectra of PE24H-AEDANS and eEF-2-AF.** The absorbance spectra of PE24H-AEDANS (*A*) and eEF-2-AF (*B*) were normalized at 280 nm. The fluorescence excitation (*solid line*) and emission spectra (*dashed line*) of PE24H-AEDANS (6.0 μM; λ_{em} = 480 nm and λ_{ex} = 337 nm for the excitation and emission spectra, respectively) (*C*) and eEF-2-AF (3.5 μM; λ_{em} = 515 nm and λ_{ex} = 492 nm for the excitation and emission spectra, respectively) (*D*) were normalized to the corresponding peak maximum values. The emission and excitation slits were both set to 2 nm. Other conditions were as described under "Experimental Procedures."

assessed when PE24H-AEDANS was chemically denatured with urea (Fig. 3*B*). PE24H-AEDANS is completely unfolded in 4 M urea (25); however, eEF-2-AF, a more structurally stable protein, remains in its native folded state at this denaturant concentration (data not shown). As shown by the data in Fig. 3*B*, no FRET occurs between denatured PE24H-AEDANS and folded eEF-2-AF, thereby providing evidence that the FRET assay is a good measure of the specific nature for the association between the toxin and eEF-2.

The *inset* to Fig. 3*B* shows a decrease in the fluorescence intensity at 460 nm as the concentration ratio of eEF-2-AF and PE24H-AEDANS approaches unity with no further change once the stoichiometry is about 2.5:1 (eEF-2:PE24H). These findings are indicative of a specific interaction between the two proteins characterized by tight binding. Binding constants for this protein-protein interaction were determined (Table II) and ranged from 0.8 to 1.9 μM for the various labeled mutant proteins.

Effect of NAD$^+$ on eEF-2 Binding to the Toxin—Using this FRET-based assay, the requirement of NAD$^+$ for the binding of eEF-2 to PE24H was also assessed. To form a stable PE24H-eEF-2-NAD$^+$ complex that is incapable of completing the transferase reaction, the nonhydrolyzable analogue of NAD$^+$, β-TAD, was used. The binding of eEF-2 to PE24H was examined both in the absence and presence of β-TAD. The similarity in the binding isotherms (Fig. 3*B*) was indicative that PE24H does not require NAD$^+$ in order to associate with eEF-2. The eEF-2 binding constants were determined to be 2.7 ($\pm$ 0.3) and 1.9 ($\pm$ 0.2) μM, respectively, for the presence and absence of β-TAD.

Interaction of PE24H with eEF-2—The effect of KCl concentration on the interaction between PE24H and eEF-2 was also investigated. Surprisingly, eEF-2 binding to PE24H was not significantly influenced by increases in KCl concentration (Fig. 4*A*), with the K_D varying only slightly, from 2.0 to 1.3 μM, for S585C-AEDANS binding with the translocase protein, which represents a 1.5-fold increase in affinity. Similarly, Na_2SO_4 and NaF had no influence on the association of these proteins (data not shown). Therefore, the protein-protein interaction that is such an integral part of the catalytic mechanism of the PE24H enzyme is not sensitive to the ionic strength of the solution.

The pH profile for eEF-2 binding to PE24H (Fig. 4*B*) shows a typical bell-shaped curve, which was fit to a Gaussian function. Notably, the pH dependence of this association could not be determined close to the pI for eEF-2 (5.0–5.3) due to its pre-

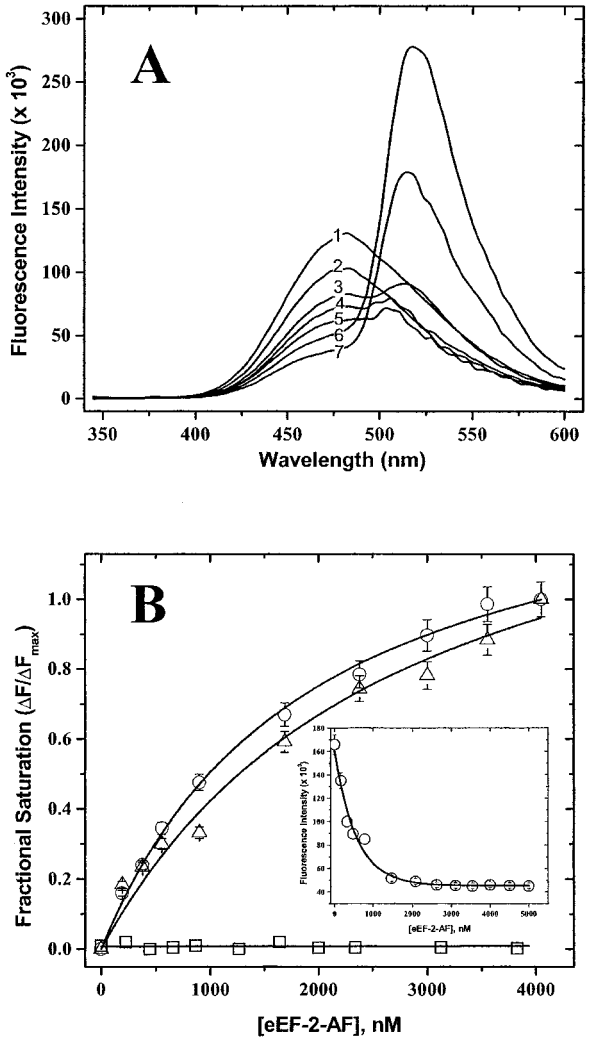

FIG. 3. **Fluorescence resonance energy transfer between PE24H-AEDANS and eEF-2-AF.** *A*, detection of FRET between PE24H-AEDANS and eEF-2-AF upon formation of the specific protein-protein complex (*curves 1–7* represent the addition of 0, 0.19, 0.55, 0.9, 1.7, 2.4, and 3.0 μM eEF-2-AF with 1.0 μM PE24H-AEDANS). The excitation wavelength was 337 nm. *B*, the binding isotherms are shown for PE24H-AEDANS only (*open circles*) in the presence of β-TAD (*open triangles*) or 4 M urea (*open squares*). The raw fluorescence quenching data were converted to fractional saturation values ($\Delta F/\Delta F_{max}$; see "Experimental Procedures") and are plotted against the 5-AF-labeled eEF-2 concentration. *Inset*, the fluorescence quenching curve for the titration of PE24H-AEDANS with eEF-2-AF. The excitation was 337 nm, and the emission was 460 nm with both excitation and emission band passes at 4 nm in 50 mM NaCl, 20 mM Tris-HCl (pH 7.9) at 25 °C. Other conditions for the experiments were as described under "Experimental Procedures."

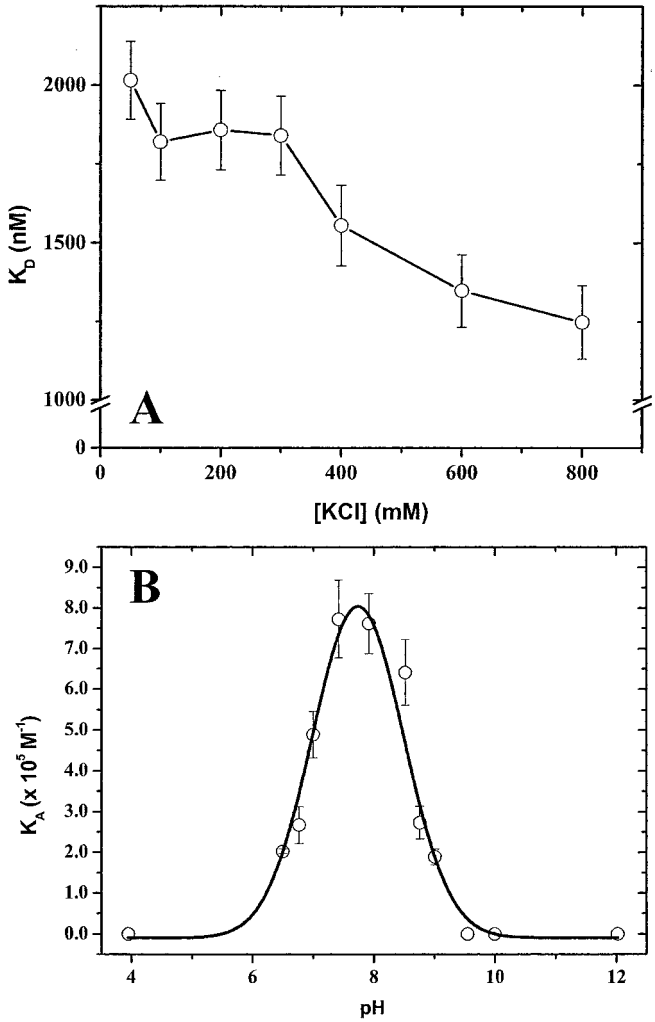

FIG. 4. **Physiological conditions for eEF-2 binding to PE24H as deduced using FRET.** *A*, eEF-2 binding as a function of KCl concentration. PE24H-AEDANS was incubated in various salt concentrations in 20 mM Tris-HCl (pH 7.9). *B*, the effect of pH on eEF-2 binding to PE24H. The pH profile for PE24H-AEDANS was generated using a series of buffers. The buffers contained 50 mM NaCl and the following buffering components: pH 4, 30 mM sodium acetate; pH 6.5–6.8, 30 mM bis-Tris, pH 7–8.8, 30 mM Tris-HCl; pH 9–12, 30 mM CAPS. The K_D values were converted to K_A values for plotting purposes. At pH 7.9, the K_A value of 7.62×10^5 M^{-1} is equivalent to a K_D value of 1300 nM or 1.3 μM. Other conditions were as described under "Experimental Procedures."

cipitation, as previously observed when assessing the pH dependence for catalytic function (21). The pH optimum for eEF-2 binding to the toxin is at 7.8 and has two pK_a values. The acidic and alkaline pK_a values are 6.3 and 9.3, respectively. Moreover, the binding affinity was negligible at pH values less than 4 and greater than 10.

eEF-2, known to bind both GTP and GDP, possesses a conserved G-core domain, which is believed to be involved in the binding and hydrolysis of GTP (26). Therefore, we investigated whether the binding of these nucleotides to eEF-2 had any effect on its ability to interact with and to be recognized by the toxin. Initially, the binding of the nonhydrolyzable analogues of GDP/GTP to eEF-2 was evaluated by monitoring the quenching of the intrinsic fluorescence of eEF-2 upon titration of these nucleotides (data not shown). The decrease in fluorescence intensity of eEF-2 indicated an association of these nucleotides with eEF-2 at the saturating concentration of 50 μM, which is in agreement with the earlier findings of Sontag *et al.* (23). As Fig. 5 illustrates, the toxin bound eEF-2-AF regardless of whether GTP-γ-S or GDP-β-S was bound to the protein substrate. The binding constants for eEF-2-AF, eEF-2-AF-GTP-γ-S, and eEF-2-AF-GDP-β-S with PE24H-AEDANS were determined to be 2.0 ($\pm$ 0.3), 1.6 ($\pm$ 0.2), and 2.1 ($\pm$ 0.3) μM, respectively. In addition, when eEF-2 was preincubated with either GTP-γ-S or GDP-β-S, the ADPRT activity of the toxin remained constant, indicating that eEF-2 in the absence or presence of bound guanyl nucleotides can still serve as a substrate for PE24H (Table III).

DISCUSSION

All cysteine-labeled PE24H mutants in this study generally behaved similarly to the wild-type enzyme and gave similar binding constants for eEF-2. Initially, this observation was perplexing because some mutants, namely T442C-, S449C-,

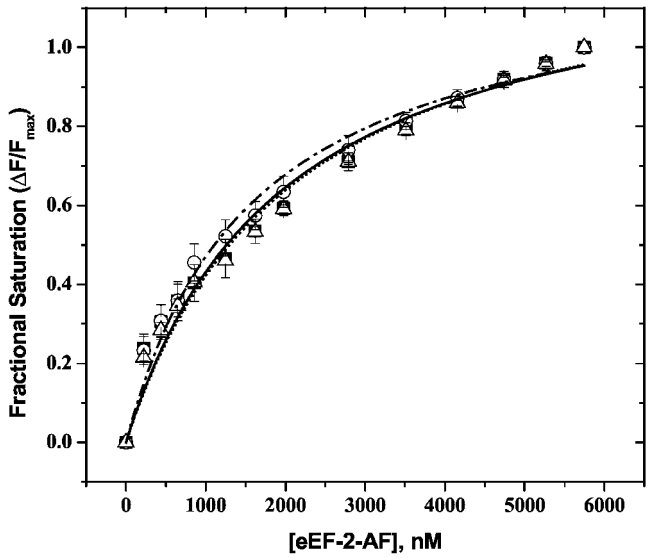

FIG. 5. **The effects of guanyl nucleotides on the binding of eEF-2-AF to PE24H-AEDANS protein.** The quenching of the AEDANS fluorescence of PE24H-AEDANS was determined from a titration of the protein adducts with native 5-AF-labeled eEF-2 (*open squares*), 5-AF-labeled-GTP-γ-S-eEF-2 (*open circles*), or 5-AF-labeled-GDP-β-S-eEF-2 (*open triangles*) as described under "Experimental Procedures." The fluorescence excitation was 337 nm, and emission was 460 nm (5 nm band passes) at 25 °C. The raw fluorescence quenching data were converted to fractional saturation values ($\Delta F/\Delta F_{max}$) and are plotted against the 5-AF-labeled eEF-2 concentration. Both GTP-γ-S and GDP-β-S were at 50 μM.

TABLE III
Comparison of the relative ADPRT activity for wild-type PE24H with the various conformational states of eEF-2

eEF-2 substrate	Relative ADPRT[a]
	%
Native-absence of bound nucleotides	100 ± 9[b]
β-GDP bound	102 ± 4
γ-GTP bound	92 ± 10

[a] The kinetics were determined as described under "Experimental Procedures" and represent the mean ± S.D. of three independent experiments. ε-NAD^+ (500 μM) and eEF-2 (14 μM) were held at saturating concentrations, and the reaction was initiated with 5 nM wild-type toxin.

[b] The 100% ADPRT activity correlates to a k_{cat} value of 1525 ± 168 min^{-1} for wild-type PE24H.

and E486C-AEDANS, all exhibited decreased catalytic function (Table II), which, in part, put into question the structural integrity of these proteins. However, when PE24H-AEDANS is completely denatured with urea and eEF-2-AF remains in its native conformation, binding is undetectable (Fig. 3*B*). Therefore, if PE24H proteins are unfolded or perhaps misfolded, they will be unable to associate, and hence no FRET will occur. This gave credence to this FRET assay as an approach to detecting a specific interaction between toxin and eEF-2 and eliminated the possibility of a fluorophore-fluorophore binding artifact. Therefore, although some of the labeled mutants had modified ADPRT activity, they still maintained the ability to bind the eEF-2 substrate. Furthermore, it might be expected that the interaction of these two proteins would involve a large number of hydrogen bonds, as well as electrostatic and Van der Waals interactions, and that modification of a single site within the toxin-enzyme would not have a significant impact on the stability of the association complex. The binding constant for the toxin-eEF-2 association was ~1 μM (Table II), which agrees with earlier findings using analogue-incorporated toxin (27).

A significant finding in the results herein is that the NAD^+ substrate is not essential for the toxin binding with eEF-2, as shown in Fig. 3*B*. Regardless of the presence or not of the dinucleotide substrate, the two proteins still associate to form a complex of similar stability. This is in agreement with previous work both using the analogue-based FRET assay (27) and through immunoprecipitation experiments (28). Interestingly, NAD^+ had previously been shown to be essential in assays based on immobilized eEF-2 (12, 29). However, the FRET-based assays represent measurements where the proteins are in solution under conditions whereby ADPRT activity can be detected, and thus these data would be expected to more representative of the *in vivo* behavior for these proteins. This new insight into this enzyme reaction suggests that the ADPRT catalytic mechanism is a random order type, in which binding of either substrate, NAD^+ or eEF-2, occurs followed by the binding of the other substrate. Previously, the reaction was proposed to follow a compulsory order mechanism (11, 12); in light of these new findings, a new enzymatic reaction model is required.

The PE24H ADPRT activity has previously been shown to be sensitive to the ionic strength of the reaction mixture, with the toxin-enzyme capable of normal catalytic function at KCl concentrations less than 100 mM (21, 30), and yet the NAD^+-PE24H interaction is only modestly dependent on salt concentration (21). It was proposed earlier that the observed salt effect on the activity of PE24H might be a reflection of the influence of ionic strength on the electrostatic interactions involved with eEF-2 (21). However, in the present study, it was shown that the binding event is relatively insensitive to salt levels (Fig. 4*A*). When the salt concentration was increased to 800 mM, at which level catalytic activity is completely absent (21), relatively little salt dependence for toxin-eEF-2 binding was observed. This is an important finding suggesting that the catalytic residues within the toxin active site are sensitive to electrostatic screening by ions and that the critical catalytic steps likely involve charged substituents within the transition state species for the ADPRT reaction.

This is also the first report that the toxin-eEF-2 interaction is highly dependent on pH (Fig. 4*B*). This dependence shows a bell-shaped relationship with a pH optimum near 7.8, an acidic pK_a value near 6.3, and an alkaline pK_a value near 9.3. Remarkably, this pH binding profile is very similar to the pH dependence observed for the catalytic activity of the toxin (21). Therefore, this pH dependence for activity may be correlated with the eEF-2 binding event. Furthermore, these pK_a values may give insight into important eEF-2 binding residues within the toxin. The acidic pK_a value is similar to that usually found for histidine. His-440 has been implicated in eEF-2 binding. However, before the work herein was done, the evidence has been circumstantial. Although His-440 is situated at the base of the active site, its ionization state may be critical for the interaction with the eEF-2 protein substrate. The alkaline pK_a may be attributed to Tyr-481, which stacks with the nicotinamide portion of the NAD^+ substrate (11), is situated near the site of cleavage within NAD^+, and thus may play an integral part in the transferase event of the catalytic mechanism (8). Moreover, both Tyr-481 and His-440 are highly conserved among diphthamide-targeting ADPRT enzymes (9, 11).

When eEF-2 associates with GTP, a conformational change is induced in the GTP-binding domain of eEF-2. This allows eEF-2 to bind to the pre-translocation ribosome with high affinity. The protein then translocates the growing peptide, which is coupled to the hydrolysis of GTP to GDP. The post-translocation ribosome has a lowered affinity for eEF-2 bound with GDP, thereby releasing this elongation factor from the ribosome (31). Using the intrinsic fluorescence of eEF-2, it has been shown that eEF-2 interacts with GDP, GTP, and their

nonhydrolyzable analogues in the absence of ribosomes (23). It was investigated whether the catalytic domain of ETA required a specific conformation of eEF-2 for protein-protein binding to occur. As the results indicate, the toxin did not prefer a specific state of eEF-2 (Fig. 5). Therefore, the toxin is able to bind eEF-2-GTP as it approaches the ribosome before forming the pre-translocation complex, as well as after it has departed the ribosome once GTP has been hydrolyzed. Earlier work using autoradiography had suggested that when NAD^+ and diphtheria toxin (a catalytically similar toxin to ETA) is added to GTP-bound eEF-2, the factor is not ribosylated (32). However, the present work showed that the presence of bound guanyl nucleotides to eEF-2 did not alter the enzyme reaction rate compared with native eEF-2 (Table III). The discrepancy between the two sets of results may rest with the method used for charging the eEF-2 protein with guanyl nucleotides. In the earlier work, *o*-GTP was used as an affinity label, which can be light-activated to covalently label the GTP-binding site. In the present study, the guanyl nucleotide analogues were simply used at saturating levels in order to populate the GTP-binding site. It is possible that the *o*-GTP affinity label induced a conformational change within the rat liver eEF-2, which may have compromised this protein as a substrate for diphtheria toxin. Alternatively, there may be a differential response for rat liver eEF-2 and wheat germ eEF-2 toward the bacterial enzymes in response to charging with guanyl nucleotides.

Dumont-Miscopein *et al.* (33) investigated the properties of two fragments produced from rat liver eEF-2 digested with endoproteinase Glu-C. The N-terminal fragment of eEF-2, which contains the G-domain, maintained its ability to interact with both GTP and GDP, and the C-terminal fragment of eEF-2 was ADP-ribosylated by diphtheria toxin. Because the C-terminal fragment lacks the G-domain, it suggests that this fragment is not governed by the conformational effects of bound guanyl nucleotides and that the critical features within eEF-2 required for toxin recognition and modification are situated within the C terminus of eEF-2. The indifference of PE24H-AEDANS for native or guanyl bound eEF-2-AF for both binding and catalytic activity further supports this conclusion (Fig. 5 and Table III). Thus, these results suggest that the protein substrate, eEF-2, is susceptible to toxin attack during its entire GTP/GDP-ribosome cycle. The only stage at which association is prevented is likely to be when the ternary complex eEF-2-GTP-ribosome forms because it has been established that ADP-ribosylation of eEF-2 cannot occur here. However, the diphthamide becomes accessible again after the lower affinity complex, eEF-2-GDP-ribosome, is produced (19). It is believed that ADP-ribosylated eEF-2 is incapable of forming the pre-translocation ternary complex, thereby preventing protein synthesis (16).

In summary, a strategy using a series of single cysteine mutants of the catalytic domain of ETA labeled with the AEDANS fluorophore in conjunction with fluorescein-labeled eEF-2 has been developed, using FRET, to provide additional insight into the nature of this protein-protein interaction. This approach has already provided a more detailed understanding of the parameters that govern the PE24H-eEF-2 association. The indifference toward NAD^+ for the enzyme-eEF-2 association process has demonstrated that the current model for the catalytic reaction may, in fact, not be a compulsory order mechanism but rather a random order type of mechanism. The pH-dependent toxin-eEF-2 association observed here is similar to the dependence seen for ADPRT catalytic function, thereby suggesting a correlation. Finally, the finding that eEF-2 bound to either GTP or GDP is still recognized as a substrate by the toxin illustrates how highly adaptable this enzyme-toxin is in its mission to ADP-ribosylate eEF-2. Future work is currently under way to elucidate in further detail the location of specific eEF-2-binding sites within the catalytic domain of ETA using this FRET-based and site-specific cysteine-scanning approach.

Acknowledgments—We thank Dr. Victor Marquez for providing the β-TAD compound used in these studies. We also express appreciation to Gerry Prentice for expert technical assistance, including the purification of eEF-2, during the course of this work.

REFERENCES

1. Vasil, M. L. (1986) *J. Pediatr.* **108,** 800–805
2. Van Delden, C., and Iglewski, B. H. (1998) *Emerg. Infect. Dis.* **4,** 551–560
3. Domenighini, M., and Rappuoli, R. (1996) *Mol. Microbiol.* **21,** 667–674
4. Althaus, F. R., and Richter, C. (1987) *Mol. Biol. Biochem. Biophys.* **37,** 1–237
5. Beattie, B. K., Prentice, G. A., and Merrill, A. R. (1996) *Biochemistry* **35,** 15134–15142
6. Sanyal, G., Marquis-Omer, D., Gress, J. O., and Middaugh, C. R. (1993) *Biochemistry* **32,** 3488–3497
7. Beattie, B. K., and Merrill, A. R. (1996) *Biochemistry* **35,** 9042–9051
8. Yates, S. P., and Merrill, A. R. (2001) *J. Biol. Chem.* **276,** 35029–35036
9. Allured, V. S., Collier, R. J., Carroll, S. F., and McKay, D. B. (1986) *Proc. Natl. Acad. Sci. U. S. A.* **83,** 1320–1324
10. Wedekind, J. E., Trame, C. B., Dorywalska, M., Koehl, P., Raschke, T. M., McKee, M., FitzGerald, D., Collier, R. J., and McKay, D. B. (2001) *J. Mol. Biol.* **314,** 823–837
11. Li, M., Dyda, F., Benhar, I., Pastan, I., and Davies, D. R. (1995) *Proc. Natl. Acad. Sci. U. S. A.* **92,** 9308–9312
12. Kessler, S. P., and Galloway, D. R. (1992) *J. Biol. Chem.* **267,** 19107–19111
13. Li, M., Dyda, F., Benhar, I., Pastan, I., and Davies, D. R. (1996) *Proc. Natl. Acad. Sci. U. S. A.* **93,** 6902–6906
14. Oppenheimer, N. J., and Bodley, J. W. (1981) *J. Biol. Chem.* **256,** 8579–8581
15. Giovane, A., Servillo, L., Quagliuolo, L., and Balestrieri, C. (1987) *Biochem. J.* **244,** 337–344
16. Nygård, O., and Nilsson, L. (1990) *Eur. J. Biochem.* **191,** 1–17
17. Mattheakis, L. C., Shen, W. H., and Collier, R. J. (1992) *Mol. Cell. Biol.* **12,** 4026–4037
18. Iglewski, W. J. (1994) *Mol. Cell. Biochem.* **138,** 131–133
19. Lavergne, J. P., Marzouki, A., Reboud, A. M., and Reboud, J. P. (1990) *Biochim. Biophys. Acta* **1048,** 231–237
20. Perentesis, J. P., Phan, L. D., Gleason, W. B., LaPorte, D. C., Livingston, D. M., and Bodley, J. W. (1992) *J. Biol. Chem.* **267,** 1190–1197
21. Armstrong, S., and Merrill, A. R. (2001) *Anal. Biochem.* **292,** 26–33
22. Steer, B. A., and Merrill, A. R. (1995) *Biochemistry* **34,** 7225–7233
23. Sontag, B., Reboud, A. M., Divita, G., Di Pietro, A., Guillot, D., and Reboud, J. P. (1993) *Biochemistry* **32,** 1976–1980
24. Wu, P., and Brand, L. (1994) *Anal. Biochem.* **218,** 1–13
25. Beattie, B. K., and Merrill, A. R. (1999) *J. Biol. Chem.* **274,** 15646–15654
26. Gonzalo, P., Sontag, B., Lavergne, J. P., Jault, J. M., and Reboud, J. P. (2000) *Biochemistry* **39,** 13558–13564
27. Mohammadi, F., Prentice, G. A., and Merrill, A. R. (2001) *Biochemistry* **40,** 10273–10283
28. Elzaim, H. S., Chopra, A. K., Peterson, J. W., Goodheart, R., and Heggers, J. P. (1998) *Infect. Immun.* **66,** 2170–2179
29. Prentice, G. A., and Merrill, A. R. (1999) *Anal. Biochem.* **272,** 216–223
30. Carroll, S. F., and Collier, R. J. (1988) *Mol. Microbiol.* **2,** 293–296
31. Nilsson, L., and Nygård, O. (1988) *Eur. J. Biochem.* **171,** 293–299
32. Nilsson, L., and Nygård, O. (1985) *Eur. J. Biochem.* **148,** 299–304
33. Dumont-Miscopein, A., Lavergne, J. P., and Reboud, J. P. (1995) *Biochim. Biophys. Acta* **1263,** 221–227
34. Lukac, M., and Collier, R. J. (1988) *Biochemistry* **27,** 7629–7632
35. Han, X. Y., and Galloway, D. R. (1995) *J. Biol. Chem.* **270,** 679–684